

Hyperfine-changing transitions in $^3\text{He II}$ and other one-electron ions by electron scattering

Klaus Bartschat¹

Department of Physics and Astronomy, Drake University, Des Moines, Iowa, 50311, USA

`klaus.bartschat@drake.edu`

and

H. R. Sadeghpour

ITAMP, Harvard-Smithsonian Center for Astrophysics, Cambridge, MA 02138, USA

`hrs@cfa.harvard.edu`

ABSTRACT

We consider the spin-exchange (SE) cross section in electron scattering from $^3\text{He II}$, which drives the hyperfine-changing 3.46 cm (8.665 GHz) line transition. Both the analytical quantum defect method — applicable at very low energies — and accurate R-matrix techniques for electron- He^+ scattering are employed to obtain SE cross sections. The quantum defect theory is also applied to electron collisions with other one-electron ions in order to demonstrate the utility of the method and derive scaling relations. At very low energies, the hyperfine-changing cross sections due to $e\text{-He}^+$ scattering are much larger in magnitude than for electron collisions with neutral hydrogen, hinting at large rate constants for equilibration. Specifically, we obtain rate coefficients of $K(10\text{ K}) = 1.10 \times 10^{-6} \text{ cm}^3/\text{s}$ and $K(100\text{ K}) = 3.49 \times 10^{-7} \text{ cm}^3/\text{s}$.

1. Introduction

The signature of matter formation, the epoch of recombination, is recorded on the relic radiation, the cosmic microwave background (CMB). This imprint occurred at the surface of last scattering, corresponding to a redshift of $z \approx 1100$. Stars ionized matter much

¹ITAMP, Harvard-Smithsonian Center for Astrophysics, Cambridge, MA 02138, USA

later, not until $6 < z < 30$ (Barkana & Loeb 2011). Observations of Lyman- α (Ly- α) absorption at $z \approx 6$ in quasars have pinned the end of the reionization epoch (Fan et al. 2002). This epoch, called the cosmic reionization, is frontier astronomy, because there are few observational constraints on the nature of processes during this era. A possible relic radiation from the reionization era could come from the hydrogen hyperfine 21-cm (1.420 GHz) tomography (Loeb & Zaldarriaga 2004), when the spin temperature of the 21-cm line (T_s) (Purcell & Field 1956) falls below that of the CMB radiation (T_{cmb}), rendering the high redshift 21-cm signal visible in the CMB.

The hyperfine transition in atomic hydrogen, and also in singly-ionized He ($^3\text{He II}$), occurs through the $F = 1 \rightarrow 0$ transition. This spin-changing transition can occur either via Raman scattering of red-shifted stellar ultraviolet light (into Ly- α resonance, the so-called Wouthuysen-Field effect (Barkana & Loeb 2005)), by collisions due to **spin dipole-dipole interaction**, or by electron scattering. The process of radiation scattering brings the photons into Boltzmann equilibrium with the surrounding gas, and hence the spin temperature into equilibrium with the gas kinetic temperature, T_k . The equilibration defines a unique spin temperature. It has been shown that collisional dipolar **processes (Zygelman 2005) are** ineffective in the redistribution of hyperfine level populations into statistical equilibrium. On the other hand, **electron-induced SE cross sections can be orders of magnitude larger than those resulting from dipolar collisions** and can readily lead to equilibration.

The hyperfine-changing transition in $^3\text{He}^+$ at 3.46 cm (8.665 GHz) is used for precise determination of the $^3\text{He}/\text{H}$ abundance in the interstellar medium (Bania et al. 1997). The source of ionization includes H II regions and planetary nebulae. ^3He can be a proxy for probe of cosmology as well as stellar and galactic evolution. In models to obtain the $^3\text{He}/\text{H}$ ratio, care must be taken to include non-LTE (local thermal equilibrium) effects and line broadening due to electron collisions (Balsler et al. 1995). As will be demonstrated below, low-energy SE collision of e^- - $^3\text{He II}$ has a much larger cross section than SE collision of e^- -hydrogen or neutral-neutral hydrogen. This is due to the presence of the long-range Coulomb interaction, which changes the energy dependence of the cross section substantially.

Spin-exchange effects in highly charged ions are also of interest for many storage ring experiments. Calculations using the Coulomb-Born and static exchange approximation, both in nonrelativistic and relativistic form, were carried out by Augustin et al. (1989). They focused on the angle-integrated spin-exchange cross section (Dalgarno and Rudge 1965)

$$\sigma_{\text{SE}} = \frac{\pi}{k^2} \sum_{\ell=0}^{\infty} (2\ell + 1) \sin^2(\delta_{\ell}^t - \delta_{\ell}^s) \quad (1)$$

for elastic collisions, where k and ℓ denote the electron's linear and angular momenta while

the superscripts on the short-range potential phase shifts, δ_ℓ^t and δ_ℓ^s , refer to triplet (t) and singlet (s) scattering with total electron spin $S = 1$ or $S = 0$, respectively. For the above definition to make physical sense, the HFS splitting (about 3.5×10^{-5} eV, corresponding to a temperature of about 0.4 K) should be small compared to the collision energy. **For the purposes intended here, this condition is well fulfilled.**

In this work, we calculate the SE cross sections for scattering of electrons from He^+ and other one-electron ions with low to intermediate nuclear charges of $2 \leq Z \leq 26$. We treat the problem in a nonrelativistic framework, but for this formulation we employ much more sophisticated methods of treating the collision process, including a convergent R-matrix (close-coupling) with pseudostates (RMPS) model that is expected to provide cross sections with an uncertainty of a few percent (in the worst scenario) for the energy range considered here. Unless specified otherwise, atomic units are used throughout this paper.

2. Numerical Methods

The collision calculations for electron scattering from He^+ were performed using the R-matrix approach (Burke 2011) as a means to solve the resulting close-coupling equations. We performed one set of calculations in a simple three-state model (to be referred to as RM-3 below), only coupling the $(1s)^2S$, $(2s)^2S$, and $(2s)^2S$ states of He^+ . This model was then extended to a 23-state RMPS approach (RM-23) based on the general method outlined in Bartschat et al. (1996). Here we added the physical $n = 3$ states plus a number of pseudostates to approximate the effect of the higher-lying Rydberg states as well as the ionization continuum on the numerical predictions. This model has been tested in great detail on several occasions, including the description of the initial bound state and the ejected-electron–residual-ion interaction in calculations of electron-impact ionization (Sakelashvili et al. 2005; Bellm et al. 2006; deHarak et al. 2014).

It is also possible to study SE in electron–ion collisions by invoking Quantum Defect Theory (QDT). Specifically, the quantum defect, i.e., the difference $\mu_\ell \equiv n - n_\ell^*$ between the effective quantum number n_ℓ^* and the nominal quantum number n in the Rydberg formula for the binding energies,

$$E_{nl} = -\frac{1}{2} \frac{Z^2}{n_\ell^*}, \quad (2)$$

is a measurement for the deviation from the pure Coulomb potential of a nuclear charge $Z - 1$ due to the imperfect screening by the inner $1s$ electron. For $n \rightarrow \infty$, the quantum defect will converge to $\bar{\mu}_\ell$, which is related to the potential scattering phase shift δ_ℓ at the

elastic threshold of zero energy via (Friedrich 2006)

$$\lim_{E \rightarrow 0} \delta_\ell(E) = \pi \bar{\mu}_\ell. \quad (3)$$

For the practical purposes of interest here, the quantum defect is sufficiently converged by $n \approx 6$, and we will see that the energy dependence of the phase shift is smooth over a relatively large energy range – except, of course, when resonances will come into play. Consequently, if accurate energy levels are available (preferably taken from experiment, but a reasonably sophisticated theory would also be appropriate), one can estimate the spin-exchange cross section to a high degree of accuracy without actually performing an extensive numerical calculation. In fact, as will be illustrated in the next section, scaling relations and the fast convergence of the results can be explained in a straightforward way using QDT arguments.

3. Results

Figure 1 shows the short-range potential phase shifts from a 23-state RMPS calculation. Note the virtually perfect agreement with what one would expect from QDT at zero energy; there is only a very weak dependence on the electron energy. Also, due to the centrifugal barrier, only partial waves with small angular momentum (in practice $\ell = 0$ and $\ell = 1$) will “see” a significant deviation of the actual potential from the ideal $Z - 1$ Coulomb potential, where one of the nuclear charges has been fully screened by the inner $1s$ electron.

Figure 2 shows the quantum defects for two-electron systems as a function of the nuclear charge Z , based on the database of the Opacity Project (Badnell et al. 2014). As mentioned above, the quantum defect is a measure of imperfect screening due to the inner $1s$ electron. Consequently, one would expect this effect to be inversely proportional to the nuclear Z , except perhaps for relatively small Z . As seen from the figure, this expectation is very well fulfilled. It then follows from Eq. (3) that the phase shifts should also fall off like $1/Z$ with increasing Z , and hence one would expect the SE cross section to scale like $1/Z^2$. This scaling relation was derived by Augustin et al. (1989) based on the properties of their specific numerical model, but we note here that this is a general feature grounded in the underlying physics.

Figure 3 shows the spin-exchange cross section for e-He⁺ scattering as a function of the electron energy. Not surprisingly, the numerical results from the 23-state RMPS model are in excellent agreement with the QDT predictions, even though the latter are, in principle, only valid at zero energy. They can, of course, not explain the strong energy dependence due to the series of Rydberg resonances starting at energies around 20 eV. The calculations

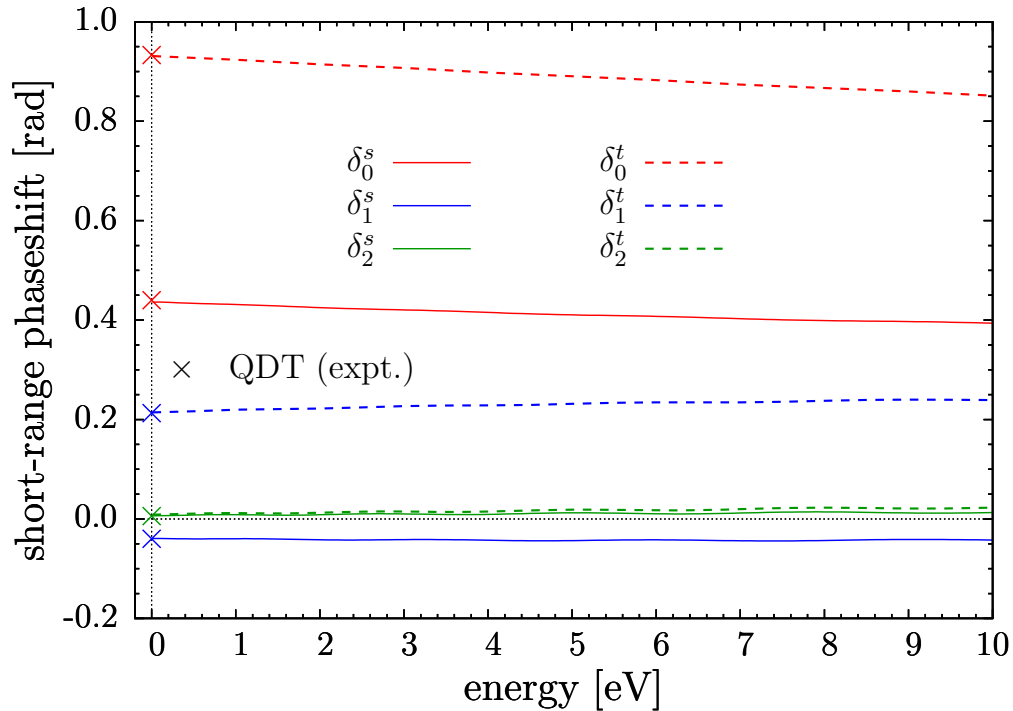


Fig. 1.— Potential phase shifts for elastic electron scattering from He^+ from a 23-state RMPS calculation. There is virtually perfect agreement with what one would expect from quantum defect theory (indicated by the crosses at $E = 0$). The quantum defects were estimated from the energy levels of the NIST database (Kramida et al. 2012). See the electronic edition of the Journal for a color version of this figure.

were performed for angular momenta up to $\ell = 4$, but they are converged – to the thickness of the line – by only accounting for $\ell = 0$ and $\ell = 1$. As already mentioned above, this fast convergence of the partial-wave expansion is a straightforward consequence of the centrifugal barrier, which leads to small quantum defects and, therefore, small short-range potential scattering phases. The long-range Coulomb phase, responsible for an infinite total cross section for elastic electron–ion scattering, is spin independent, and hence it cancels out when the difference in the spin phase shifts is taken.

Once again considering practical applications, we notice that the results from the three-state model already appear to be accurate within a few percent. This shows that describing electron scattering even from a singly ionized target is significantly easier than the corresponding problem of collisions with a neutral hydrogen atom (Bartschat et al. 1996).

Figure 4 shows the QDT results for elastic electron collisions with He^+ and selected other one-electron ions up to Fe^{25+} . In this case, the quantum defects were taken from

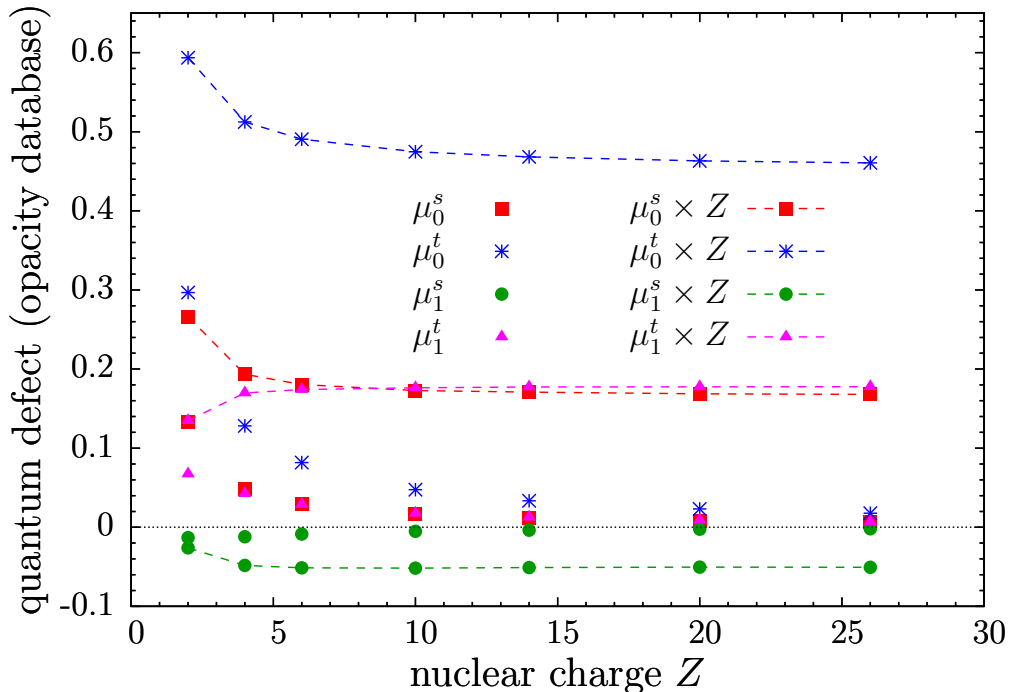


Fig. 2.— Quantum defects for two-electron systems as a function of the nuclear charge Z , based on the database of the Opacity Project (Badnell et al. 2014). The quantum defects scale as $1/Z$, as one would expect, with a slight deviation for small Z . See the electronic edition of the Journal for a color version of this figure.

the database of the Opacity Project (Badnell et al. 2014). Even though it is difficult to accurately read numbers off their graphs, there are significant deviations between our results and those of Augustin et al. (1989). While this may be understandable for the He^+ target, one would expect much better agreement for the highly charged ions.

We finish with a comparison of the SE cross section for neutral hydrogen and He^+ . The predictions are shown in Fig. 5 for energies below the first negative-ion resonance in e–H collisions. The hydrogen results were obtained using the highly accurate phase shifts of Schwartz (1961) for the s-wave and Bhatia (2004) for the p-wave. [Similar results, using slightly different phaseshifts, were published by Furlanetto & Furlanetto (2007). Note, however, that their definition of the spin-exchange cross section (see Eq. 10 of the paper) differs from ours in Eq. (1) above by a factor of 4.]

In addition to plotting the SE cross section, we also show it multiplied by the energy (taken in eV in order to ensure good visibility on the graph). Due to the QDT scaling for an ionic target such as He^+ , the cross section grows proportional to $1/E$ for $E \rightarrow 0$. For

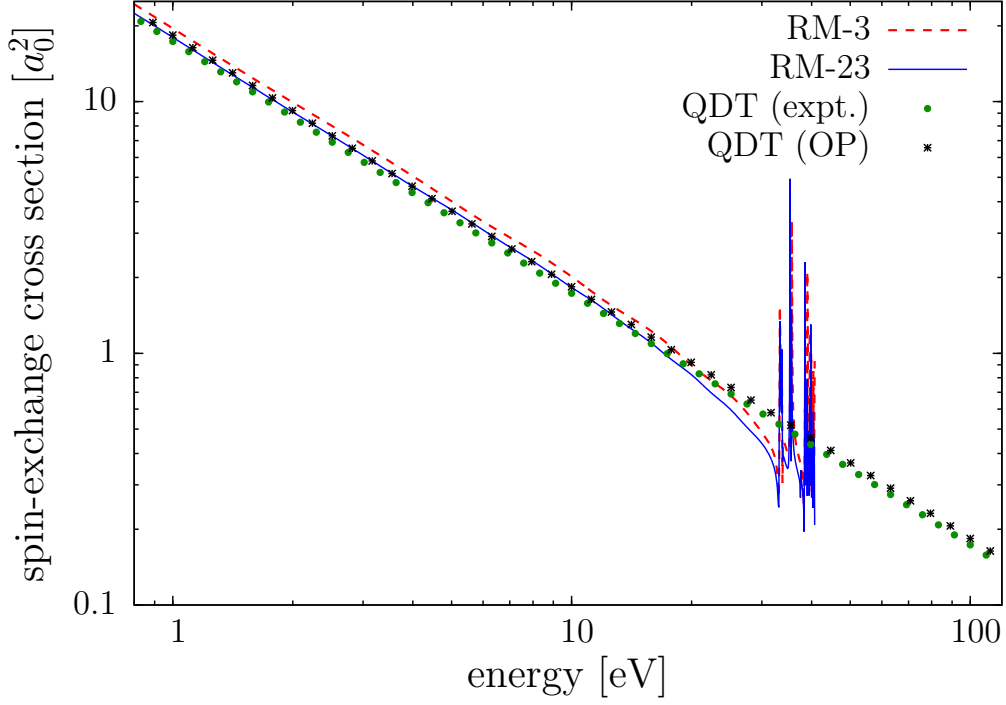


Fig. 3.— Spin-exchange cross section for $e\text{-He}^+$ scattering as a function of the electron energy. Numerical results from a 23-state RMPS model are compared with predictions from a much simpler 3-state approach, as well as QDT results obtained with quantum defects from experiment (Kramida et al. 2012) or the opacity database (Badnell et al. 2014). The inverse linear dependence with energy of the SE cross sections, as predicted from the QDT analysis is confirmed in the numerical calculations. See the electronic edition of the Journal for a color version of this figure.

neutral hydrogen, on the other hand, low-energy collisions are dominated by the polarization potential. The threshold behavior is very different, as seen most clearly when the cross section is multiplied by the energy. Specifically, the spin-exchange cross section for neutral hydrogen will approach the finite value of

$$\lim_{E \rightarrow 0} \sigma_{\text{SE}}(E) = \pi(a^t - a^s)^2, \quad (4)$$

where a^t and a^s are the scattering lengths for triplet and singlet scattering, respectively.

Finally, the collisional rate coefficients are:

$$K(T) = \sqrt{\frac{8k_B T}{\pi m}} \int_0^\infty \sigma(\bar{E}) e^{-\bar{E}} d\bar{E}, \quad (5)$$

where m is the electron mass, T is the temperature in K, k_B is the Boltzmann constant, and $\bar{E} \equiv E/(k_B T)$. Given the $1/E$ dependence of the SE cross section for $e\text{-He}^+$ collisions, with

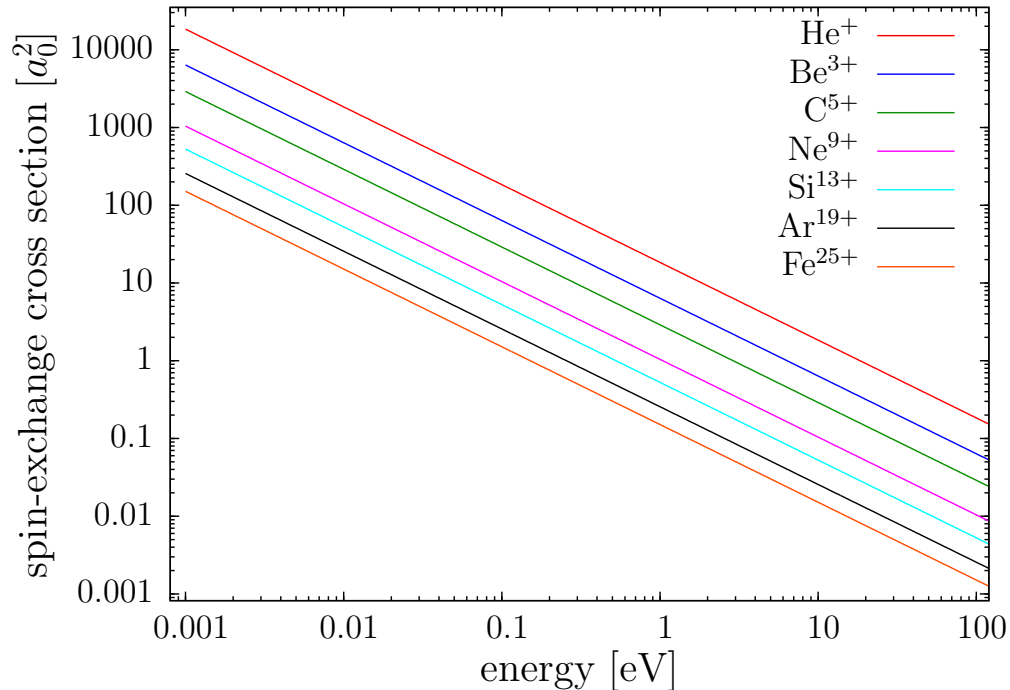


Fig. 4.— Spin-exchange cross sections predicted from QDT results obtained with quantum defects from the Opacity Project database (Badnell et al. 2014). See the electronic edition of the Journal for a color version of this figure.

a slope of $17.3 a_0^2 \times \text{eV}$, we obtain the explicit form

$$K(T) = 3.49 \times 10^{-6} T^{-1/2} \text{cm}^3/\text{s}. \quad (6)$$

This yields, for example, $K(T = 10 \text{ K}) = 1.1 \times 10^{-6} \text{cm}^3/\text{s}$ and $K(T = 100 \text{ K}) = 3.49 \times 10^{-7} \text{cm}^3/\text{s}$. The enormous rate coefficients in the scattering of electrons from ${}^3\text{He II}$ are due to the fact that the SE cross section scales as $1/E$ and hence is infinite at zero energy.

4. Summary

We have presented short-range phase shifts and spin-exchange cross sections for elastic electron scattering from selected one-electron ions from He^+ to Fe^{25+} . The results were explained in a simple physical picture based on quantum defect theory. In the low-energy range, which is of particular interest for astrophysical applications, it seems unnecessary to perform explicit numerical calculations for the scattering process, as long as accurate quantum defects are available. Our results differ significantly from those published previously, partly due to the more sophisticated approach used in the present work (for small Z) and

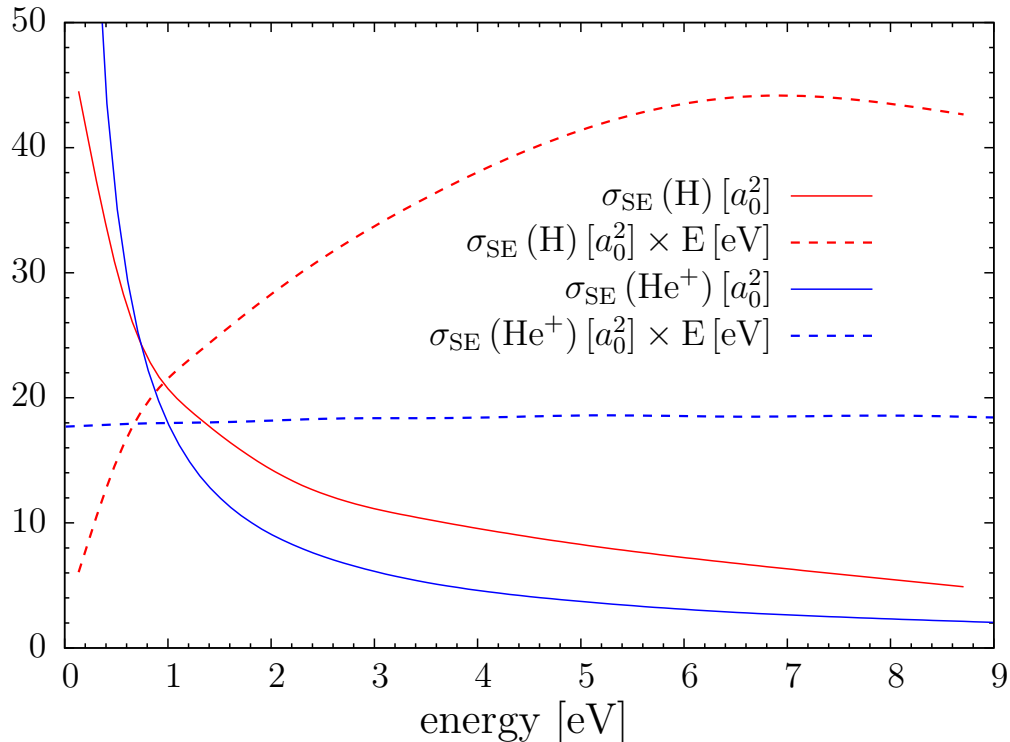


Fig. 5.— Spin-exchange cross sections for He^+ (obtained from the RM-23 model) and neutral atomic hydrogen. The latter were obtained using phase shifts from Schwartz (1961) for the s-wave and Bhatia (2004) for the p-wave. Also shown are the cross sections multiplied by the energy (in eV), in order to show the entirely different energy dependence, in particular at very low energies. See the electronic edition of the Journal for a color version of this figure.

partly due to a possible plotting error in Augustin et al. (1989). The entirely different energy dependence of the spin-exchange cross section for ionic versus neutral targets leads to very large rate coefficients for the electron-induced 3.46 cm line transition in $^3\text{He II}$ at low temperatures.

Acknowledgments

This work was supported by the United States National Science Foundation under grant No. PHY-1068140 (KB) and through a grant to the Institute for Theoretical Atomic, Molecular and Optical Physics at Harvard University and the Harvard-Smithsonian Center for Astrophysics.

REFERENCES

- Augustin, J., Müller, B., & Greiner, W. 1989, *Z. Phys. D* 14, 312
- Badnell, N. et al. 2014, The Iron Project – The Opacity Project,
<http://cdsweb.u-strasbg.fr/topbase/energy.html>
- Bania, T. M. et al. 1997, *ApJ Suppl. Ser.* 113, 353
- Balser, D. S., Bania, T. M., Rood, R. T., & Wilson, T. L. 1995, *AJ* 100, 371
- Barkana, R., & Loeb, A. 2011, *Phys. Rep.*, 349, 125
- Barkana, R., & Loeb, A. 2005, *AJ* 626, 1
- Bartschat, K., Hudson, E. T., Scott, M. P., Burke, P. G., & Burke, V. M. 1996, *J. Phys. B* 29, 115
- Bellm, S., Lower, K., & Bartschat, K. 2006, *Phys. Rev. Lett.* 96, 223201
- Bhatia, A. K. 2004, *Phys. Rev. A* 69, 032714
- Burke, P. G. 2011, *R-Matrix Theory of Atomic Collisions*, Springer: Berlin
- Dalgarno, A., & Rudge, M. R. H. 1965, *Proc. Roy. Soc. London A* 286, 519
- deHarak, B. A., Bartschat, K., & Martin, N. L. S. 2014, *Phys. Rev. A* 89, 012702
- Fan, X., Narayanan, V., Strauss, M., White, R., Becker, R., Pentericci, L., & Rix, H. 2002, *AJ* 123, 1247
- Friedrich, H. 2006, *Theoretical Atomic Physics (3rd edition)*, Springer: Berlin
- Furlanetto, S. R. & Furlanetto, M. R., *MNRAS* (2007) 374, 547
- Kramida, A., Ralchenko, Yu., Reader, J. et al. 2012, NIST Atomic Spectra Database (Version 5); <http://www.nist.gov/pml/data/asd.cfm> (Gaithersburg: National Institute of Standards and Technology).
- Loeb, A. & Zaldarriaga, M. 2004, *Phys. Rev. Lett.* 92, 211301
- Purcell, E. M., & Field, G. B. 1956, *AJ* 124, 542
- Sakelashvili, G., Dorn, A., Höhr, C., Ullrich, J., Kheifets, A., Lower, J. & Bartschat, K. 2005, *Phys. Rev. Lett.* 95, 033201

Schwartz, C. 1961, Phys. Rev. 124, 1468

Zygelman, B. 2005, AJ 622, 1356